Analysis of fatigue crack propagation and crack shielding in super duplex stainless steel and its welds

Karel Slámečka[1,a], Guocai Chai [2,b] and Jaroslav Pokluda[1,c]

[1]Brno University of Technology, Faculty of Mechanical Engineering, Technická 2893/2, Brno, Czech Republic

[2]Sandvik Materials Technology, R&D center, 811 81 Sandviken, Sweden

slamecka@fme.vutbr.cz[a], [b]guocai.chai@sandvik.com, [c]pokluda@fme.vutbr.cz

Keywords: Fatigue crack propagation, Fatigue crack closure, Fatigue crack branching, Duplex stainless steels, Welds.

Abstract. Fatigue crack propagation behaviour in super duplex austenitic-ferritic stainless steel and its weld was analysed. ΔK-decreasing tests were performed and the fatigue crack growth rate (FCGR) data were generated. Fatigue crack closure was evaluated by processing the mechanical compliance data stored during the experiments. Fatigue crack branching was assessed based on the edge-filtering of high resolution light optical microscopy images. Although the comparison of the crack behaviour in the base material and the welded material was complicated by an irregular crack path within the welded specimen, distinctive differences of all evaluated characteristics were observed.

Introduction

Super duplex stainless steels (SDSS) are the alloys with a fine grained ferritic-austenitic microstructure, high mechanical strength and fracture toughness and an excellent resistance to stress corrosion cracking. Such properties designate SDSS for utilization in aggressive environments with severe corrosion conditions as frequently encountered in chemical and petrochemical industry or marine applications. In both these areas, welding is most often employed as a joining method for its high productivity and performance.

Although the fatigue crack data are available in a form of a well-known Wöhler curve (the nominal stress versus a number of cycles to failure), it is well known that this characteristic does not distinguish between the fatigue crack initiation and propagation stages and gives no information on a crack growth process. As in reality the pre-existing flaws or/and crack-like defects might reduce or even completely eliminate the initiation phase, such additional information as the fatigue crack growth threshold, the fatigue crack growth rate, the extend of crack closure and branching and the understanding of mechanisms involved are required in order to design reliable components and structures and to prevent their failure by specifying a safe service inspection interval in a frame of the fail-safe design approach.

Material and experimental procedure

Material studied herein is a highly alloyed super duplex stainless steel SAF 2507 (equivalent to UNS S32750) with a nominal chemical composition given in Table 1. Material was supplied in the form of a hot-rolled bars from which the compact tension C(T) specimens of width W=36 mm and thickness B=18 mm were machined in a TS-orientation (see the ASTM E399 standard). Welds were produced by Tungsten Inert Gas (TIG) welding technique. In this method a tungsten electrode is used to form the arc. The electrode and the weld pool are shielded by inert gas and the filler rod is fed into the weld pool separately. The welding direction was parallel to the S-direction, which also is the expected direction of the fatigue crack propagation, Fig. 1.

Table 1. Nominal chemical composition of SAF 2507 (wt%).

C	Si	Mn	Cr	Ni	Mo	N	Fe
0.03	0.8	1.2	25	7	4	0.3	balance

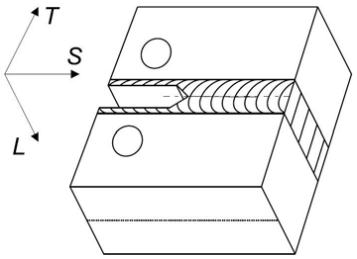

Fig.1. The location and the orientation of the weld.

Microstructure of the base material consists of approximately equal amount of both ferrite and austenite with austenitic grains elongated in the rolling direction, Fig. 2. Microstructure of the welded material contains slightly higher amount of ferritic phase in the weld. The structure of austenitic grains within the weld and the heat-affected zone (HAZ) differs significantly from that of the base material, Fig. 3. Tensile properties of the base material in the rolling direction are summarized in Table 2, where σ_y is the yield strength and σ_u denotes the tensile strength.

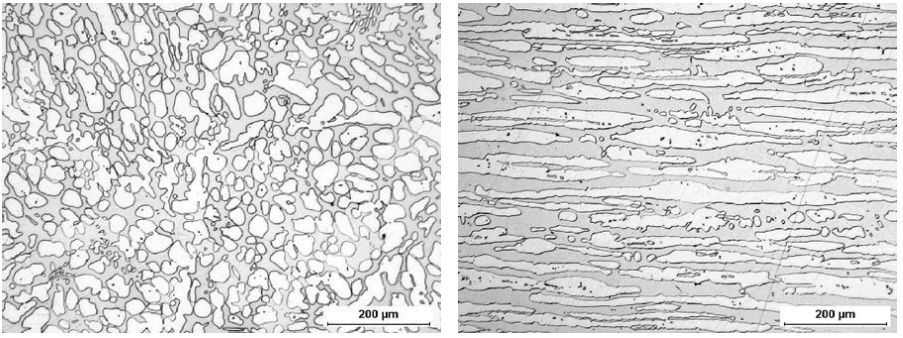

Fig.2. Microstructure of the base material: the elongated austenite grains are in a continuous ferrite matrix (electroetching in 25% nitride acid).

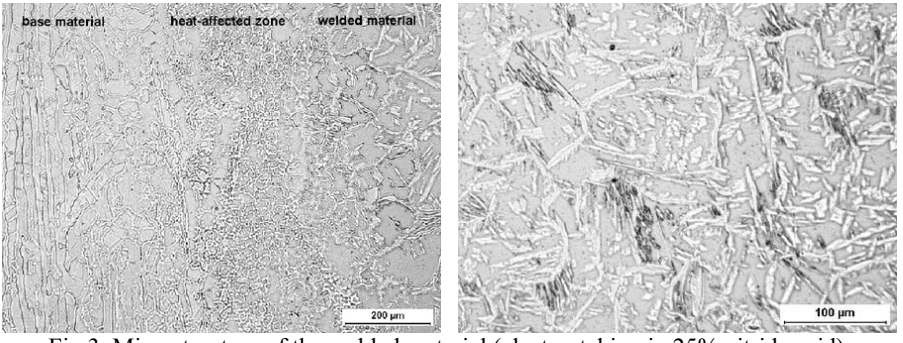

Fig.3. Microstructure of the welded material (electroetching in 25% nitride acid).

Table 2. Tensile properties of SAF 2507 in the rolling direction.

Temperature [C°]	σ_y [MPa]	σ_u [MPa]	Elongation [%]
20	625	820	41.7

The fatigue crack growth rate (FCGR) tests were carried out under load-control conditions by means of a MTS servo-hydraulic testing system equipped with a 50 kN loading cell and Instron 8500+ digital electronics. `Fast Track Program da/dN' software provided by Instron was used to control the experiments and to store results [1]. Prior to testing, specimens were pre-cracked in order to provide sharp and straight initial fatigue crack of an adequate size following the methodology suggested in the ASTM E647-05 standard [2].

Continuous ΔK-decreasing procedure was used as a loading regime. In accordance with the ASTM E647-05 standard, initial values of ΔK and K_{max} for experiments were always higher than the terminal ΔK and K_{max} values of the pre-cracking procedure. Sinusoidal varying loading of frequency 10 Hz and the loading ratio R=0.1 was applied for both the pre-cracking and the experiments. Tests were conducted in air at the room temperature 20 °C. The normalized K-gradient,

$$C_g = \left(\frac{1}{K}\right)\left(\frac{\mathrm{d}K}{\mathrm{da}}\right) = -0.10\,\mathrm{mm}^{-1}, \tag{1}$$

was used as the load shedding parameter. As recommended by the standard, both the loading ratio, R, and the normalized K-gradient, C_g, were kept constant during experiments. The determination of the crack size, a, during the experiment was carried out by processing of the mechanical compliance data from the crack opening displacement gauge located on the notch mouth. The compliance was evaluated for loads between 50% and 90% of the total load-COD curve. The resolution of the method was 0.01 mm.

Two specimens machined from the hot-rolled bars coming from the same batch are studied herein. Specimen B was made from the base material; specimen W was prepared with the weld. The analysis of the crack path within the specimen B shows that the crack propagated in more or less planar manner with only minor deviations from the expected crack plane. On the other hand, the examination of the specimen W revealed variations in the weld thickness as well as transient departure of the crack out from the weld into HAZ, Fig. 4. After experiments, specimens were saw-cut into two parts, one of which was used for the crack-size rectification. The second part of the specimen was moulded into bakelite and prepared by standard procedures for a crack path observation.

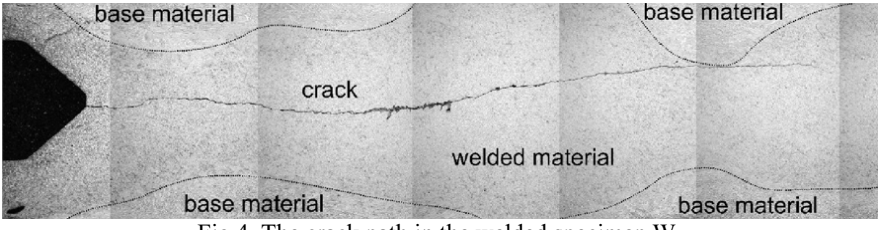

Fig.4. The crack path in the welded specimen W.

Results and discussion

Sets of fatigue crack growth rate data were generated by means of the in-house code `fcgr'. Results are shown as Fig. 5a. As can be seen, base-material specimen B shows the typical threshold behaviour with the fatigue crack growth rate, da/dN, almost reaching the conventional threshold level of 10^{-7} mm/cycle. In a case of the welded specimen W, an irregular fatigue crack growth rate is observed. Starting with decreasing da/dN at the beginning of the test at higher ΔK-level, a transient plateau is reached followed by further decrease of the fatigue crack growth rate. At loading level of $\Delta K \approx 12$ MPa.m$^{0.5}$, the propagation speed increases suddenly continuing afterwards again in expected deceleration. While in the first case it is not easy to explain the crack growth behaviour, in the later case the change in the crack propagation dynamics corresponds to the crack length $a \approx 29$ mm, which is the region in which the crack departures temporarily out of the centre of the weld into HAZ, Fig. 4. Thus, the irregular crack growth is almost certainly attributed to the change of the conditions on the crack front herein.

The fatigue crack growth threshold, ΔK_{th}, was estimated as the best fit straight line from a linear regression of bilogaritmic FCGR data, i.e., log(da/dN) vs. log (ΔK), in the crack growth rate range of da/d$N \in (10^{-6}, 10^{-7})$ mm/cycle. In the case of the specimen B (base material), the fatigue crack growth threshold $\Delta K_{th} = 5.7$ MPa.m$^{0.5}$ was found. In the case of the specimen W, fatigue crack growth threshold was evaluated for each decreasing branch separately. The calculated results are $\Delta K_{th(1)} = 11.7$ MPa.m$^{0.5}$ (higher-ΔK branch) and $\Delta K_{th(2)} = 9.5$ MPa.m$^{0.5}$ (lower-ΔK branch) meaning that the fatigue crack growth threshold for the welded material is almost two times higher than the fatigue crack growth threshold obtained herein for the base material.

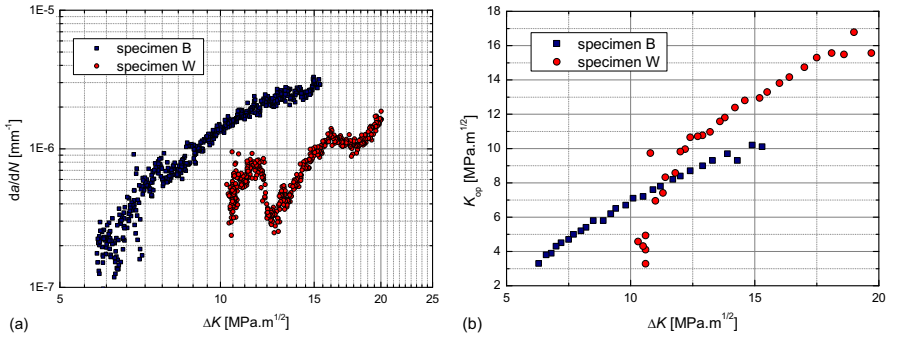

Fig.5. (a) Fatigue crack growth rate curves, (b) fatigue crack closure results expressed in terms of the opening stress-intensity factor, K_{op}.

The determination of the fatigue crack closure was done by means of the compliance method that is based on the analysis of the mechanical compliance data measured and stored during the experiments. Same data as those used for the crack length evaluation were employed; in this case, however, the whole load-COD curves were taken into account. The applied load, P, versus the crack opening displacement (COD), v, curve displays two main slopes corresponding to the regions of fully opened and fully closed crack. The crack opening load, P_{op}, is estimated as the load for which the compliance, $c = v/P$, remains constant for the fully open crack. In this work, the crack opening load, P_{op}, was identified following the procedure recommended by ASTM E647-05 standard by analysing the variations in the slope along the compliance curve. A preset deviation in the compliance offset from the fully-open value, the so-called the compliance offset criterion [2], which defines the crack opening load, P_{op}, was set to 4%.

Fatigue crack closure was expressed by means of the opening stress-intensity factor, K_{op}, which is the stress-intensity factor that corresponds to the crack opening load, P_{op}. Results are shown as

Fig. 5b, where K_{op} is plotted against the applied stress-intensity factor range, ΔK. Although a higher scatter of the compliance data signal was experienced in a case of the welded specimen W, especially at lower loads, it is concluded with a good degree of reliability that a much higher closure level than that in the case of the base material specimen B is found from the start of the experiment for almost the whole testing time. This behaviour is probably connected with very complex and extensive crack branching within the specimen W, see Table 4. At the end of the experiment, however, a rapid decrease of crack closure level is found (sudden change in the slope somewhere at $\Delta K \approx 12$ MPa.m$^{0.5}$) reaching even below the closure level within the specimen B. Although this change in the closure behaviour incidents with the time when the crack was growing out of the weld, it is difficult to explain continuingly low closure up to the end of the testing.

Evaluation of the fatigue crack branching was done by analysing high-resolution bitmap images acquired at magnification 1000× by means of the light optical microscope (LOM). Digitalized images were printed out and the crack path was traced and highlighted on printouts with the help of the edge-filtering computer algorithms applied to the original bitmap files. Examination of the specimen B revealed that there are mainly two types of branching events in the base-material: (i) `short branches' with the length $l \leq 15$ μm and (ii) long branches with the length $l \geq 30$ μm. Only a very few cracks ceased to grow at an intermediate length 15 μm $\leq l \leq$ 30 μm. The numbers of short branches together with the origin of their initiation (within the ferritic grain, within the austenitic grain, at the ferrite-austenite grain boundary) were assessed. The second parameter being evaluated was the total length fraction affected by branching, P_B, which is the parameter that enters advanced models for evaluation of the crack tip shielding, see e.g. [3,4]. The analysis of the crack path within the welded specimen was complicated by much finer microstructure and a complex crack network, which at most regions rendered the recognition of individual short branches extremely difficult. Due to this reason, only the parameter P_B was evaluated for the welded specimen W.

Two regions were analysed for each specimen. Information on location, stress intensity factor range and the fatigue crack growth rate are summarized in Table 3. Results are shown in Table 4, where N_α is the number of short branches (branches with the length lower than 15 μm) initiated within ferrite grains, N_γ is the number of short branches initiated within austenite grains, $N_{\alpha\gamma}$ is the number of short branches formed at the ferrite-austenite boundary, N_T is the total number of short branches ($N_T = N_\alpha + N_\gamma + N_{\alpha\gamma}$), and P_B is the length fraction influenced by branching.

Table 3. Fatigue crack branching – analysed regions.

Region	a [mm]	ΔK [MPa.m$^{0.5}$]	da/dN [mm/cycle]
B1	20.0-21.0	12.7-11.5	$2.1\times10^{-6} - 1.9\times10^{-6}$
B2	25.1-26.1	7.9-7.3	$5.7\times10^{-7} - 5.5\times10^{-7}$
W1	23.5-24.5	18.1-16.6	$1.6\times10^{-6} - 1.2\times10^{-6}$
W2	26.5-27.5	13.9-12.9	$7.3\times10^{-7} - 6.0\times10^{-7}$

Table 4. Fatigue crack branching – results.

Region	N_α	N_γ	$N_{\alpha\gamma}$	N_T	P_B
B1	6	24	6	36	30
B2	6	40	4	50	33
W1	-	-	-	-	71
W2	-	-	-	-	62

As it is seen from Table 4, the total number of short branches, N_T, in the base material is slightly lower for the region B2. Note, however, that more extensive analysis suggests that the parameter N_T is less sensitive to ΔK in the low ΔK-range [5]. The length fraction influenced by branching is almost the same $P_B \approx 30\%$. Furthermore, it is noted that branching occurs most frequently within

austenite grains. This result is expected to be caused by the FCC structure of austenite with higher number of slip systems available for the branch initiation. The numbers of branches generated in ferrite and at the ferrite-austenite boundary are generally low. The most interesting result of the analysis is the high difference of the length fraction influenced by branching, P_B, within the base material and the welded material. As mentioned above, this behaviour is supposed to correspond to high closure found within the welded specimen being caused by the extensive asymmetric crack-wake plasticity [6,7].

Summary

The analysis of the fatigue crack propagation in super duplex austenitic-ferritic stainless steel and its weld was performed. Although the comparison of the crack behaviour in the base material and the welded material was complicated by an irregular crack path within the welded specimen, which temporarily leaves the weld, the distinctive differences of the fatigue crack growth rate, crack shielding (closure and branching) and the fatigue crack threshold were observed. More extensive study is needed in order to refine current knowledge on the fatigue crack propagation in the SDSS and especially within the welded material, which would be able to confirm observed trends on the statistical bases.

Acknowledgement

This paper is published by permission of Sandvik Materials Technology. The authors, K. Slámečka and J. Pokluda, acknowledge the financial support provided by the Ministry of Education, Youth and Sports of the Czech Republic (projects MSM 0021630518 and NPVII-2E08017).

References

[1] G. Chai: *Evaluation of Instron Fast Track Program: da/dn, by use of SAF 2507 aged at 475℃*, Internal Report at AB Sandvik Steel, AB Sandvik Steel, Sandviken, 1998.

[2] ASTM E647-05: *Standard Test Method for Measurement of Fatigue Crack Growth Rates, Annual Book of Standards, Section 3 - Metals Test Methods and Analytical Procedures*, in: Vol. 03.01, Metals - Mechanical Testing; Elevated and Low-Temperature Tests; Metallography, ASTM, West Conshohocken, PA, 2007, 692-735.

[3] J. Pokluda, P. Šandera and J. Horníková: Fat. Fract. Engng. Mater. Struc. Vol. 27 (2004), p. 141.

[4] G. Chai and J. Pokluda, in: *Proc. Fatigue 06*, edited by W.S. Johnson, Elsevier (cd), Atlanta, Georgia, 2006, p. 0205A_06.

[5] G. Chai, R.L. Peng, K. Slámečka and S. Johansson: submitted to the ECF-17 conference.

[6] J. Pokluda, P. Šandera and R. Pippan, *Proc. Fatigue 06*, edited by W. S. Johnson, Elsevier (cd), Atlanta, Georgia, 2006, p. 0107A_03.

[7] J. Pokluda and R. Pippan: Mat. Sci. Eng. A Vol. 462 (2007), p.355.